DOI: 10.37190/ABB-02323-2023-06

Adipose derived stem cells and ginkgo biloba extract-loaded PCL/gelatin nanofibrous scaffolds for peripheral nerve injury repair: The impact of physical activity

Hua Gong [1], Zhengtian Chen [2*]

[1] School of Physical Education, Liaoning Normal University; Liaoning Dalian, 116029, China

[2] School of Physical Education and Health Science, Guangxi MinZu University; Guangxi Ningnin, 530000, China

Corresponding Author: Zhengtian Chen, School of Physical Education and Health Science, Guangxi MinZu University; Guangxi Ningnin, 530000, China, e-mail address: chenzhengtian888@163.com

Submitted: 4th October 2023

Accepted: 30th January 2024

Abstract

Peripheral nerve damages take place as a result of trauma, compression, or disease, resulting in sensory loss, impaired motor function, and subsequent challenges. In the current study, ginkgo biloba extract was loaded into PCL/gelatin scaffolds through electrospinning method. The scaffolds were characterized in vitro using various studies. The prepared nanofibrous scaffolds were rolled up to make neural guidance channels. Then, the conduits were seeded with adipose derived stem cells and transplanted into a rat model of sciatic nerve injury. The scaffolds were not toxic and had optimal tensile and suturability. The animals treated with the conduits that delivered adipose derived stem cells and ginkgo biloba extract and received the treadmill exercise had significantly higher motor and sensory functions recovery. In addition, histopathological examinations showed beneficial role of the exercise plan on the nervous system repair.

Keywords: Ginkgo biloba extract; Drug delivery; Neural conduit; Nanofibers; Electrospinning; Peripheral nervous system

1. Introduction

Peripheral nerve damages take place as a result of trauma, compression, or disease, resulting in sensory loss, impaired motor function, and subsequent challenges. Unfortunately, the regenerative capacity of peripheral nervous system tissues is limited, requiring the development of new therapeutic strategies to stimulate nerve regeneration and improve functional outcome [15, 45, 47]. Conventional treatment methods have proven to be unsatisfactory, highlighting the need for innovative approaches. Stem cells are appealing in regenerative medicine due to their unique potentials, including self-renewal, multi-lineage differentiation capability, and paracrine secretion capacity. Among the various types of stem cells, adipose-derived stem cells (ADSCs) have emerged as a potent tool in nerve regeneration research [18,35, 42, 43]. These cells are readily harvestable and accessible, and they exhibit robust regenerative potential. These cells secrete different growth factors and cytokines that promote neural cells survival, angiogenesis at the injury site, and nerve regeneration. Additionally, ADSCs can differentiate into Schwann cell-like phenotypes, making them ideal cell sources for cell-based therapies in nerve regeneration [4, 21, 42].

Biomaterial-based scaffolding systems serve as essential constructs for cells' growth, proliferation, and differentiation. Synthetic polymers such as polycaprolacton (PCL) and natural polymers like gelatin have caught attention in developing neural conduits owing to their biocompatibility, biodegradability, and customizable mechanical properties. Electrospinning method has been widely explored for developing biomimetic neural conduits [19, 8, 23, 17]. These scaffolds closely resemble the native extracellular matrix (ECM), providing an ideal microenvironment for cells' function. These scaffolds have the potential for drug delivery applications. In this regard, various bioactive agents have been loaded into their matrix. Ginkgo biloba extract (GBE), derived from the leaves of the Ginkgo biloba tree, has exhibited neuroprotective and neuro-regenerative potentials. This extract contains flavonoids and terpenoids known for their antioxidant and anti-inflammatory effects, which result in its potential beneficial therapeutic effect on nerve regeneration [33]. In this regard, Huang et al. showed that GBE mitigated neurotoxicity and promoted neural regeneration in hippocampus after exposure to acrylamide [16].

Physical rehabilitation, including exercise therapy, has shown positive effects on functional recovery following PNS injuries. Mild treadmill exercise, in particular, has been shown to promote

the production of neurotrophic factors, promote angiogenesis, and facilitate neuronal plasticity, thereby helping the nerve regeneration and functional restoration [3,6, 29, 30].

In combination, the synergistic effects of ADSCs, GBE-loaded PCL/gelatin nanofibrous scaffolds, and mild treadmill exercise may offer a promising approach for repairing peripheral nerve injuries. This innovative strategy aims to create an optimal microenvironment that promotes cell survival and differentiation, while also enhancing the release of neurotrophic factors, angiogenesis, and the establishment of functional neural connections.

2. Materials and methods

2-1. Preparation of GBE-loaded PCL/gelatin scaffolds via electrospinning

The GBE-loaded PCL)/gelatin nanofibrous scaffolds were prepared using the electrospinning technique. Initially, a PCL and gelatin blend solution was prepared by dissolving 1.4 gram of PCL (Mn 80000, Sigma Aldrich, USA) and 200 mg of gelatin (Type A, Sigma Aldrich, USA) in acetic acid (Glacial, Merck, Germany). Next, the GBE was incorporated into the PCL/gelatin solution at 10 v/v%. The solution was thoroughly blended using a magnetic stirrer for 2 hours to ensure a homogeneous distribution of the extract within the polymer blend. Once the PCL/gelatin solution with the GBE was prepared, it was loaded into a syringe fitted with a blunt needle. The electrospinning process was performed at a voltage of 18 kV using a syringe pump with a flow rate ranging from 0.5 ml/hour to 1 mL/hour. A grounded collector plate was placed at a distance of 15-16 cm from the needle tip. The electrospinning process was conducted in a controlled environment at a temperature of 25°C and a relative humidity of 40% to minimize any external disturbances that could affect the quality and morphology of the nanofibrous scaffolds. The electrospun nanofibers were deposited on an aluminium foil with dimensions around 25×20 cm^2 for 8 hours.

2-2. Scanning electron microscopy (SEM) imaging

PCL/gelatin scaffolds containing GBE and PCL/gelatin scaffolds without GBE were subjected to a gold coating process lasting 250 seconds, followed by imaging at an accelerating high voltage of 26 KV.

2-3. Cell viability assay

The metabolic activity of PC-12 cells on GBE-loaded PCL/gelatin scaffolds and GBE-free PCL/gelatin scaffolds was assessed using the MTT assay. PC-12 cells seeded on the scaffolds at a density of 5,000 cells per scaffold in a 96-well plate. The plate was then incubated at 37°C in a humidified atmosphere with 5% CO2. On day 1, 3, and 7, the culture medium was removed, and the scaffolds with adhered cells were gently washed with PBS. Then, 100 µL of MTT solution (0.5 mg/mL in culture medium, Sigma Aldrich, USA) was added to each well, and the plate was incubated for 4 hours at 37°C to allow the MTT reagent to be metabolized by the cells. After the incubation time, the MTT solution was carefully removed, and formed formazan crystals were solubilized in 200 µL of dimethyl sulfoxide (DMSO) with gentle agitation for 10 minutes. The absorbance was measured at 570 nm with a reference wavelength of 630 nm. For each time step, the viability of PC-12 cells on GBE-loaded PCL/gelatin scaffolds and GBE-free PCL/gelatin scaffolds was calculated as a percentage relative to the control group, which consisted of PC-12 cells cultured on tissue culture plate.

2-4. Anti-inflammatory assay

The anti-inflammatory activity of GBE-loaded PCL/gelatin scaffolds and GBE-free PCL/gelatin scaffolds was investigated. Briefly, Raw 264.7 macrophages were seeded onto the scaffolds at a density of 1 × 10^5 cells per scaffold in a 24-well plate. Then, cells were cultured for 24 hour and then they were stimulated with Lipopolysaccharide (1 µg/ml, Sigma Aldrich, USA). After 24 hours of incubation, the culture medium was collected, and the levels of pro-inflammatory cytokines, including TNF-α and IL-6 were measured using enzyme-linked immunosorbent assay (ELISA) kits (Abcam, USA) according to the manufacturer's instructions. To evaluate the anti-inflammatory activity, the production of TNF-α and IL-6 was compared between the GBE-loaded PCL/gelatin scaffolds and GBE-free PCL/gelatin scaffolds. The results were also compared to a positive control group consisting of macrophages stimulated with LPS but without any scaffold. The experiment was performed in triplicate, and the mean cytokine levels were calculated.

2-6. Mechanical analysis

The mechanical properties of GBE-loaded PCL/gelatin scaffolds and GBE-free PCL/gelatin scaffolds were investigated using a mechanical testing device. The scaffolds were shaped into

rectangular pieces measuring 1cm in width and 3cm in length. A total of 5 specimens were prepared for each scaffold group. Tensile tests were conducted at a constant crosshead speed of 10 mm/min until the samples reached their breaking point. Throughout the experiment, the applied load on the scaffold was continuously monitored, alongside the corresponding displacement measurements. By studying the load-displacement data, the stress-strain curve was generated, allowing for the determination of the ultimate tensile strength as the maximum stress encountered before scaffold failure.

2-7. Biodegradation rate measurement

The degradation rate of GBE-loaded PCL/gelatin scaffolds and GBE-free PCL/gelatin scaffolds was analyzed to study their biodegradation rate over a period of 60 days. Scaffolds were cut into 50-100 mg pieces. Each scaffold group consisted of 5 samples. The degradation process began by immersing the scaffold samples in 20 ml of PBS. The buffer solution was kept at a temperature of 37°C to simulate the body's internal environment. At specific time intervals, including 1 week, 2 weeks, 4 weeks, and 8 weeks, the scaffold samples were carefully retrieved from the buffer solution and gently rinsed with distilled water to eliminate any residual buffer solution. Afterward, the samples were carefully blotted dry and weighed using an analytical balance with a precision of 0.001 g. The weight loss percentage was calculated by comparing the dry weight of the matrices with their corresponding weights at each designated time point.

2-8. Surface contact angle measurement

The surface contact angle of GBE-loaded PCL/gelatin scaffolds and GBE-free PCL/gelatin scaffolds were studied using the sessile drop method. The scaffolds were cut into dimensions of 1 cm by 1 cm. First, a water droplet was carefully dispensed onto the surface of each scaffold sample using a precision micropipette. The droplet size was controlled to ensure consistency between samples. A high-resolution camera was used to captured images of the liquid droplet on the scaffold surface. The captured images were analyzed using specialized software to measure the contact angle formed at the liquid-scaffold interface. The contact angle was calculated by determining the angle between the tangent line of the liquid droplet and the solid scaffold surface. This measurement provided information about the wettability and surface hydrophilicity/hydrophobicity of the scaffolds.

2-9. Release assay

The evaluation of GBE release from PCL/gelatin scaffolds was conducted through UV-visible spectroscopy at 410 nm, corresponding to GBE's λ max in PBS. In a concise summary, 200 mg of scaffolds were immersed in PBS and incubated at 37 ºC for a duration of 10 days. At various time intervals, samples of the release medium were collected, and their optical density was measured, fitting the obtained values into the standard GBE curve. Subsequently, the cumulative release profile was computed to provide a comprehensive understanding of the release kinetics over the specified time frame.

2-10. In vivo study

A method was utilized to study the healing efficacy of different treatment approaches in a rat model of sciatic nerve injury. A total of 18 male Sprague-Dawley rats were randomly divided into six groups, with 3 rats in each group. The surgery to create the injury model was carried out under clean conditions. Anesthesia was induced by intraperitoneal injection of ketamine and Xylazine. The skin on the surgical site was prepared by shaving and disinfecting the area with betadine solution. A longitudinal incision of approximately 2 cm was created on the gluteal muscle to expose the sciatic nerve. Then, the sciatic nerve was meticulously isolated from the surrounding muscle tissues and transected completely using surgical scissors, leaving in a complete nerve gap. Great care was taken to prevent injuries to the nearby blood vessels or connective tissues. For the autograft group, a segment of the sural nerve, approximately 10 mm in length, was harvested from the rat's own sural nerve of the contralateral limb. The harvested nerve segment was immediately placed into the nerve gap, aligning the proximal and distal nerve ends. The graft was secured using 9-0 nylon sutures, ensuring a tension-free repair. In the GBEPCLGELADSCs + physical activity and GBEPCLGELADSCs groups, the conduits were implanted at the injury site and then 50000 ADSCs in 1.5 wt.% collagen hydrogel were injected into the conduit’s lumen. The scaffold was secured using 9-0 nylon sutures. For the PCLGEL + physical activity and PCLGEL groups, the conduits used in a similar manner as the GBEPCLGELADSCs groups, but without the addition of ADSCs. In the negative control group, no treatment was applied to the transected sciatic nerve. The animals were kept for 8 weeks in individual cages. During the recovery period, the animals in groups that included physical activity program, received 15 minutes treadmill exercise every two days until the end of the experiment. At the end of 8^{th} week, the animals were sacrificed and their

gastrocnemius and sciatic nerve tissues were harvested for histopathological studies using H&E and Masson's Trichrome staining.

2-11. Functional assessment methods

The motor function recovery of the animals in each group was assessed using Sciatic Functional Index (SFI) method as described before [11]. For the evaluation of gastrocnemius muscle re-innervation, additional assessments were conducted to quantify the degree of muscle atrophy and recovery. This involved harvesting the gastrocnemius muscle tissues from both the operated limb (the limb with the sciatic nerve injury) and the non-operated limb (control limb) at the end of 8th post-surgery. Immediately after harvesting, the muscle tissues were weighed to measure their wet weight. Gastrocnemius muscle from the un-injured limb acted as a reference for normal muscle mass. To assess the extent of muscle atrophy, the wet weight of the gastrocnemius muscle in the operated limb was compared to that of the non-operated limb. The percentage of gastrocnemius muscle wet weight loss was calculated using the following formula:

Percentage of wet weight loss = [(Weight of non-operated limb - Weight of operated limb) / Weight of non-operated limb] x 100

This calculation allowed for the quantification of the degree of muscle wasting or preservation in the operated limb compared to the non-operated limb. A higher percentage of wet weight loss indicated greater muscle atrophy, while a lower percentage indicated better preservation or recovery of muscle mass.

To assess the restoration of sensory function in the rat model of sciatic nerve injury, a method known as the hot plate test was utilized. This particular test aimed to measure the sensitivity of the rats' hind limbs to thermal stimulation. Individually, the rats were placed on a hot plate with a controlled temperature set at approximately 56 ºC. This temperature was chosen as it reliably evoked a response in healthy rats. To ensure the rats' safety, the surface of the hot plate was covered with a protective layer, preventing direct contact between their skin and the hot surface. The reaction time was recorded as the duration elapsed between placing the rat on the hot plate and the observable response, such as withdrawal of the paw or licking, indicating discomfort caused by the thermal stimulus. To ensure accuracy, either an infrared sensor or a stopwatch was employed

to precisely measure the reaction time. The cutoff time was set at 12 seconds. By comparing the reaction times among the different treatment groups, the efficacy of each treatment approach in facilitating sensory function recovery could be evaluated. A shorter reaction time indicated a quicker recovery of sensory function, while a longer reaction time suggested the persistence of sensory impairment.

2-12. ELISA assay

At the end of 8th week, the tissue levels of NGF and BDNF in sciatic nerve tissues were evaluated using ELISA assay kits (Abcam, USA) using a method provided by the manufacturer.

2-13. Statistical analysis

Data was analyzed using Graphpad prism version 5 via students t-test and one-way ANOVA. Each experiment was repeated at least three times. Data normality was assessed through visual inspections, including histograms and Q-Q plots, complemented by statistical tests like the Shapiro-Wilk or Kolmogorov-Smirnov tests. Homogeneity of variances, crucial for ANOVA, was examined using Levene's Test or Barlett's Test to ensure variances across groups were roughly equal. Maintaining the independence of observations focused on random sampling to prevent systematic relationships. Outlier analysis played a vital role, identifying and addressing outliers that could unduly influence results. Data transformations, like logarithmic or square root transformations, were sometimes applied to stabilize variances or enhance normality.

3. Results

3-1. SEM imaging results

The results depicted in Figure 1 provided an insightful characterization of the microstructure of electrospun PCL/gelatin scaffolds, both loaded with GBE (GBE-loaded) and without GBE (GBE-free). Microscopic analysis revealed that both types of scaffolds exhibited a fibrous structure with fibers displaying a jagged surface. The fibers appeared to be continuous without any evidence of bead formation, indicating a successful electrospinning process. To further examine the dimensions of the fibers, fiber size measurements were conducted. The average fiber size for the GBE-loaded PCL/gelatin scaffold was determined to be approximately 634.69 ± 192.65 nm. On the other hand, the GBE-free PCL/gelatin scaffold exhibited an average fiber size of around 578.3 ± 119.22 nm. These measurements indicated that the GBE-loaded scaffold had slightly larger fibers compared to the GBE-free scaffold. The fibrous microstructure of the scaffolds, characterized by continuous fibers with a jagged surface, is desirable as it offers a high surface area-to-volume ratio, which can facilitate cellular adhesion and proliferation. The absence of bead formation further indicated the uniformity and integrity of the electrospun fibers.

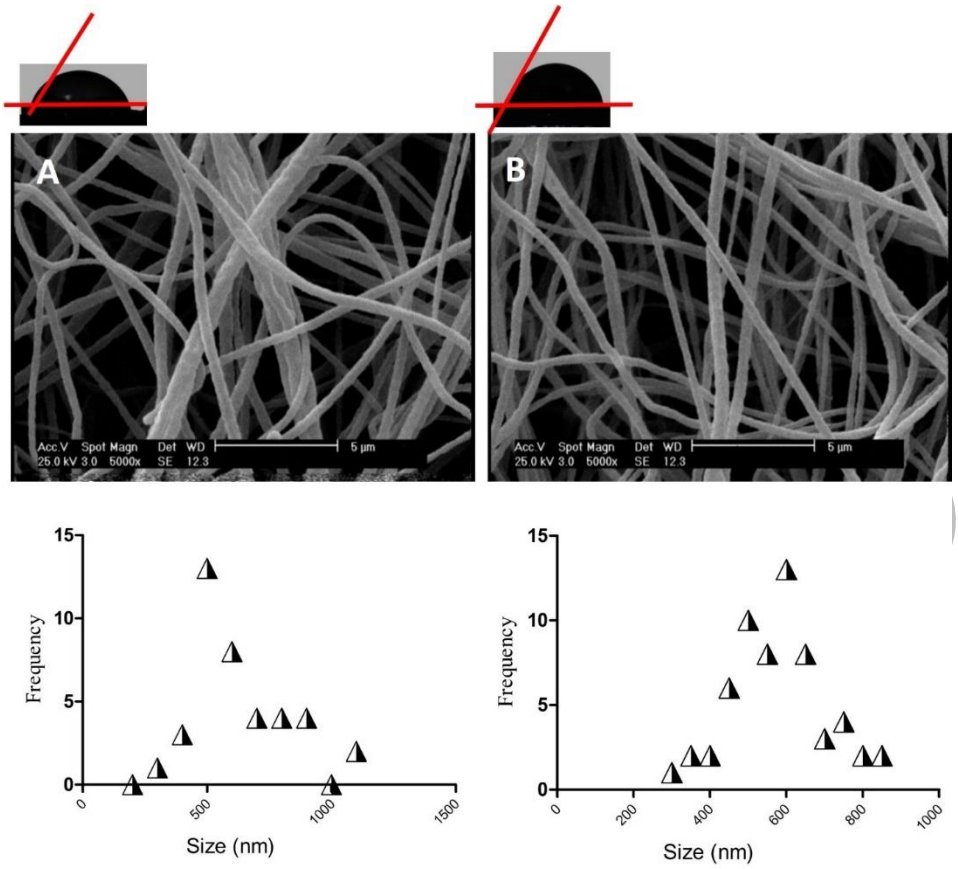

Figure 1. SEM images, water contact angle, and size distribution of (A) GBE-loaded PCL/gelatin scaffolds and (B) GBE-free PCL/gelatin scaffolds

3-2. Cell viability assay

The results obtained from the study, as depicted in Figure 2, revealed that the viability of PC-12 cells was maintained in both GBE-loaded and GBE-free PCL/Gelatin scaffolds throughout the entire duration of the experiment. The assessment of cell viability was performed at various time points, and it was observed that the cells exhibited a healthy state without any significant decline in viability. Comparing the viability of cells in control group with those cultured on the electrospun scaffold groups, no notable differences were observed. Statistical analysis, using a p-value threshold of 0.05, indicated that the disparities in viability between these two groups were not statistically significant. Therefore, based on these findings, it can be reasonably concluded that the scaffolds employed in this study did not exhibit any toxic effects on the PC-12 cells.

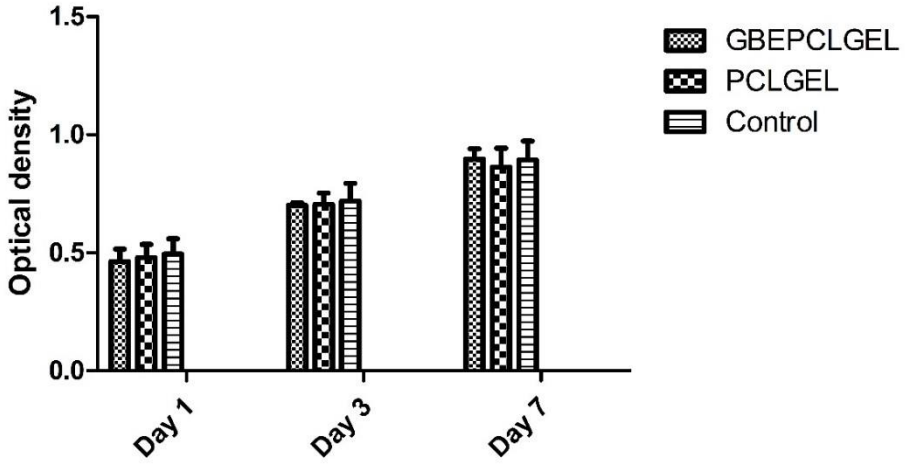

Figure 2. MTT assay with PC-12 cells cultured with GBEPCLGEL and PCLGEL scaffolds compared with cells cultured on tissue culture plate as the control group

3-4. Anti-inflammatory assay

Results (Figure 3) showed that concentrations of IL6 and TNF-a in GBEPCLGEL group was significantly lower than PCLGEL and control group, indicating that incorporation of GBE into the matrix of PCL/gelatin scaffolds has imparted immunomodulatory activity to the scaffolds.

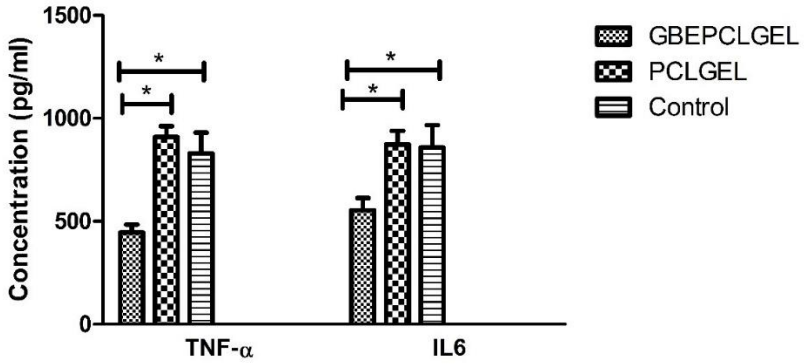

Figure 3. Anti-inflammatory assay with Raw 264.7 macrophage cells cultured on GBEPCLGEL and PCLGEL scaffolds. * Shows p-value < 0.05

3-5. Ultimate tensile strength measurement

Results showed that GBEPCLGEL and PCLGEL scaffolds had around 1.65 ± 0.18 MPa and 1.73 ± 0.21 MPa of ultimate tensile strength, respectively. Therefore, it seems that adding GBE into the electrospun scaffolds did not significantly change their mechanical properties.

3-6. Biodegradation rate measurement

Results (Figure 4A) showed that both GBEPCLGEL and PCLGEL scaffolds had a similar pattern of biodegradation. During the first 11 days of the scaffold's incubation in PBS, they experienced a relatively rapid biodegradation. Then, the rate of biodegradation slowed down and reached a plateau. At the end of 15th day, the rate of biodegradation for GBEPCLGEL and PCLGEL scaffolds was measured to be 12.19 ± 2.94 % and 11.17 ± 2.28 %, respectively. From day 15th on, the rate of biodegradation gradually increased and reached to maximum level at the end of 60th day post-incubation in PBS.

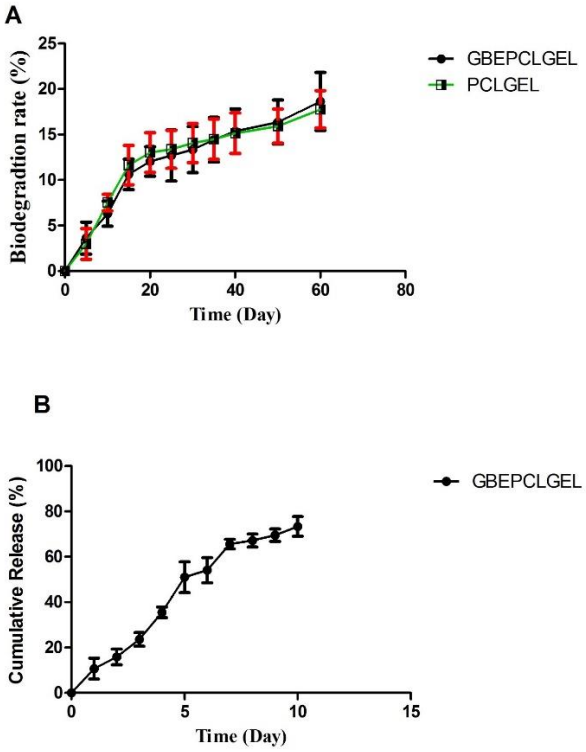

Figure 4. (A) shows Biodegradation rate of GBEPCLGEL and PCLGEL scaffolds in PBS during a 60-day incubation period and (B) shows release of GBE from the matrix of GBEPCLGEL scaffolds

3-7. Surface contact angle measurement

Results (Figure 1) showed that surface contact angle for GBEPCLGEL and PCLGEL scaffolds was around 76.18 ± 7.57 º and 77.14 ± 7.36º, respectively. Therefore, both scaffolds had a hydrophilic surface (surface contact angle < 90 º). GBE did not significantly affect scaffolds surface wettability.

3-8. Release assay results

The outcomes of the release assay (depicted in Figure 4B) demonstrated a consistent and sustained release of Ginkgo biloba extract (GBE) from the GBEPCLGEL scaffold matrix. Initially, a rapid release phase was observed, succeeded by a plateau phase persisting for over 10 days. By the 10th day, the cumulative release of GBE reached a substantial level, specifically measured at 73.37 ± 4.30%.

3-9. Histopathological examinations

The H&E and Masson's Trichrome staining images (Figure 5 and Figure 6) of the autograft nerve group exhibited the most favorable healing outcome. The gastrocnemius muscle and sciatic nerve tissues showed well-organized and intact tissue structures, with preserved cellular morphology, minimal cellular degeneration, and absence of necrosis. The H&E staining reveals normal cellular architecture, with minimal inflammatory infiltrates characterized by scattered lymphocytes and macrophages. Masson's Trichrome staining demonstrated minimal fibrosis, indicating a favorable healing process, with only a few collagens fibers present in the connective tissue. Histopathological examination images for the GBEPCLGELADSCs + physical activity group displayed a relatively positive healing response. The gastrocnemius muscle and sciatic nerve tissues showed moderate preservation of tissue architecture, with mild degenerative changes observed in a few cells. The H&E staining revealed scattered inflammatory infiltrates, consisting of lymphocytes and macrophages, indicating a mild inflammatory response. Masson's Trichrome staining indicated mild fibrosis, suggesting ongoing tissue remodeling and healing, with an increase in collagen deposition and formation of a few fibrotic areas. In the GBEPCLGELADSCs group, the H&E staining images show moderate preservation of tissue architecture in the gastrocnemius muscle and sciatic nerve tissues. However, there is a slightly higher presence of inflammatory infiltrates compared to the previous group, with increased numbers of lymphocytes and macrophages. Some degenerative changes, such as cellular swelling, were also observed. Masson's Trichrome staining displays increased fibrosis compared to the autograft nerve and GBEPCLGELADSCs + physical activity groups, indicating ongoing tissue remodeling and scar formation, with the presence of moderate fibrotic areas and collagen deposition. The H&E and Masson's Trichrome staining images of the PCLGEL + physical activity group reveal a less favorable healing response. The gastrocnemius muscle and sciatic nerve tissues show moderate

disruption of tissue architecture, characterized by extensive cellular degeneration, necrosis, and loss of cellular organization (Figure 7 and 8). Inflammatory infiltrates are prominent, consisting of a large number of lymphocytes, plasma cells, and macrophages. Masson's Trichrome staining demonstrates considerable fibrosis, indicating excessive scar formation and impaired tissue remodeling, with the presence of dense collagen fibers and fibrotic areas. The PCLGEL group showed a compromised healing response. The gastrocnemius muscle and sciatic nerve tissues exhibit significant disruption of tissue architecture, with widespread cellular degeneration, necrosis, and loss of tissue integrity. Inflammatory infiltrates are abundant, comprising a large number of lymphocytes, plasma cells, and macrophages. Masson's Trichrome staining shows extensive fibrosis, indicating the formation of dense collagen fibers and fibrotic areas throughout the tissues, suggesting impaired tissue regeneration and remodeling. The H&E and Masson's Trichrome staining images of the negative control group demonstrated the poorest healing response. The gastrocnemius muscle and sciatic nerve tissues exhibited extensive disruption of tissue architecture, characterized by severe cellular degeneration, necrosis, and loss of tissue integrity. Inflammatory infiltrates are pronounced, with a significant influx of lymphocytes, plasma cells, and macrophages throughout the tissues. Masson's Trichrome staining reveals pronounced fibrosis, indicating the formation of dense collagen fibers and extensive fibrotic areas, suggesting a failure in tissue repair and an impaired healing process exacerbated by the lack of treatment.

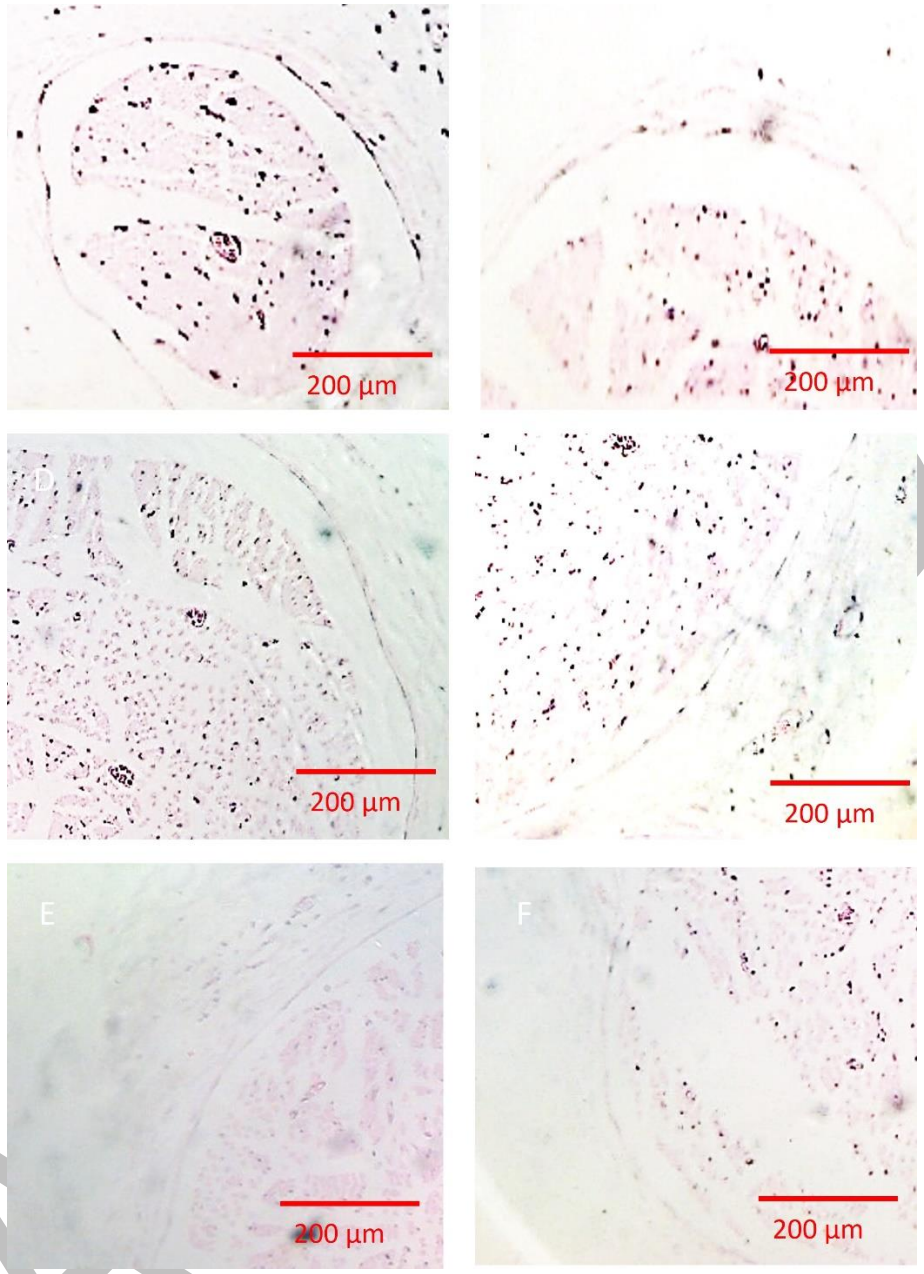

Figure 5. H&E staining images of sciatic nerve tissues in (A) autograft group, (B) GBEPCLGELADSCs + physical activity group, (C) GBEPCLGELADSCs group (D) PCLGEL + physical activity group, (E) PCLGEL group, and (F) negative control group

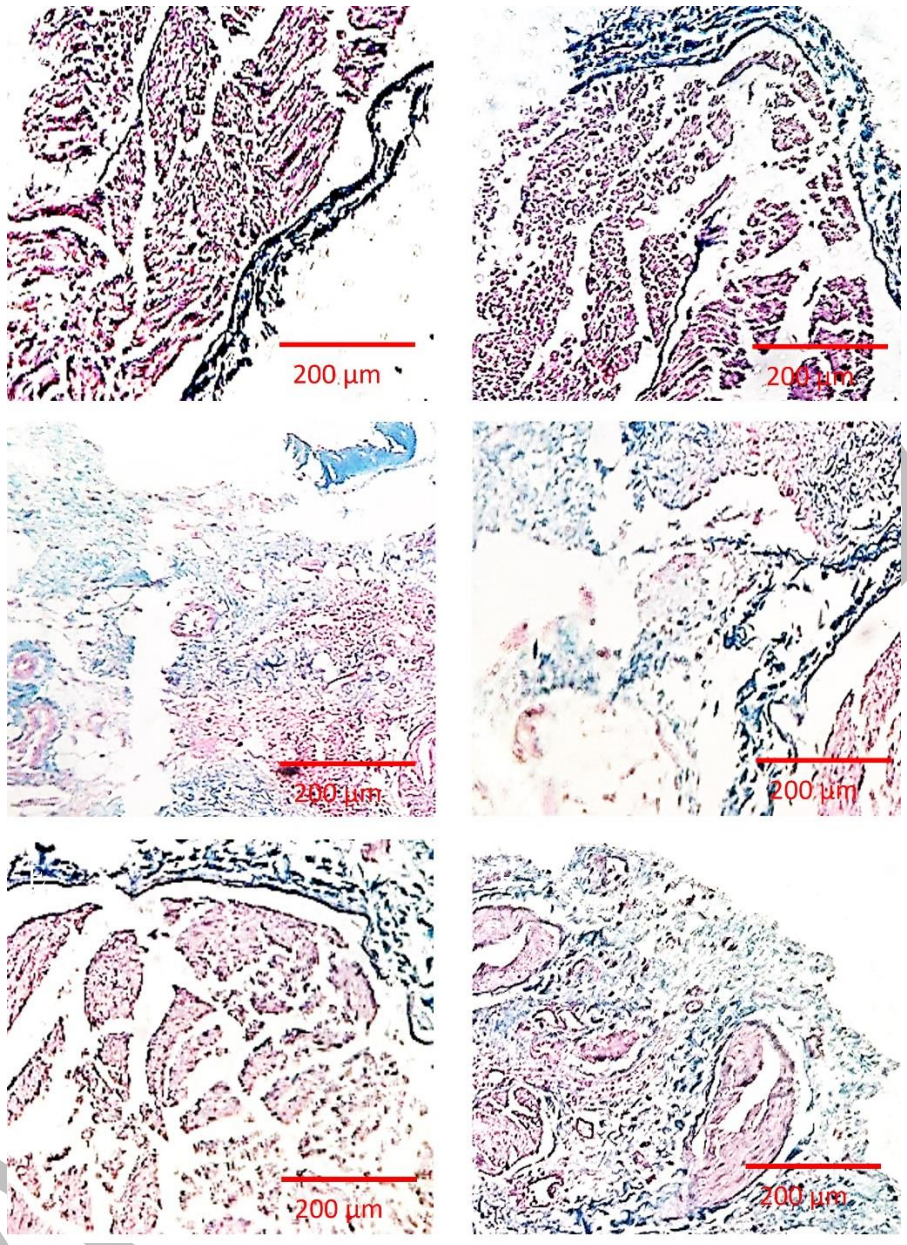

Figure 6. Masson's trichrome staining images of sciatic nerve tissue in (A) autograft group, (B) GBEPCLGELADSCs + physical activity group, (C) GBEPCLGELADSCs group (D) PCLGEL + physical activity group, (E) PCLGEL group, and (F) negative control group

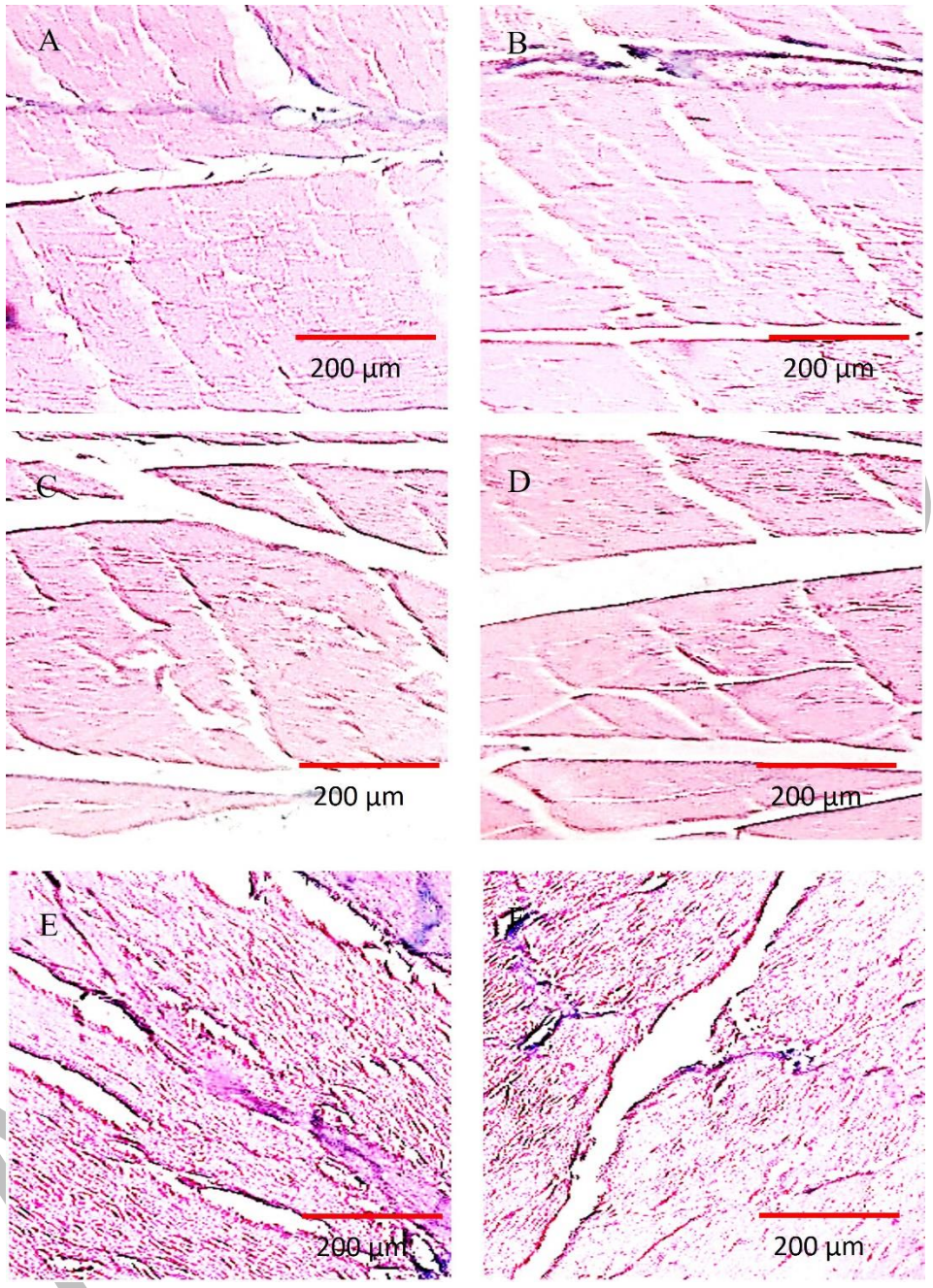

Figure 7. H&E staining images of gastrocnemius muscle tissue in (A) autograft group, (B) GBEPCLGELADSCs + physical activity group, (C) GBEPCLGELADSCs group (D) PCLGEL + physical activity group, (E) PCLGEL group, and (F) negative control group

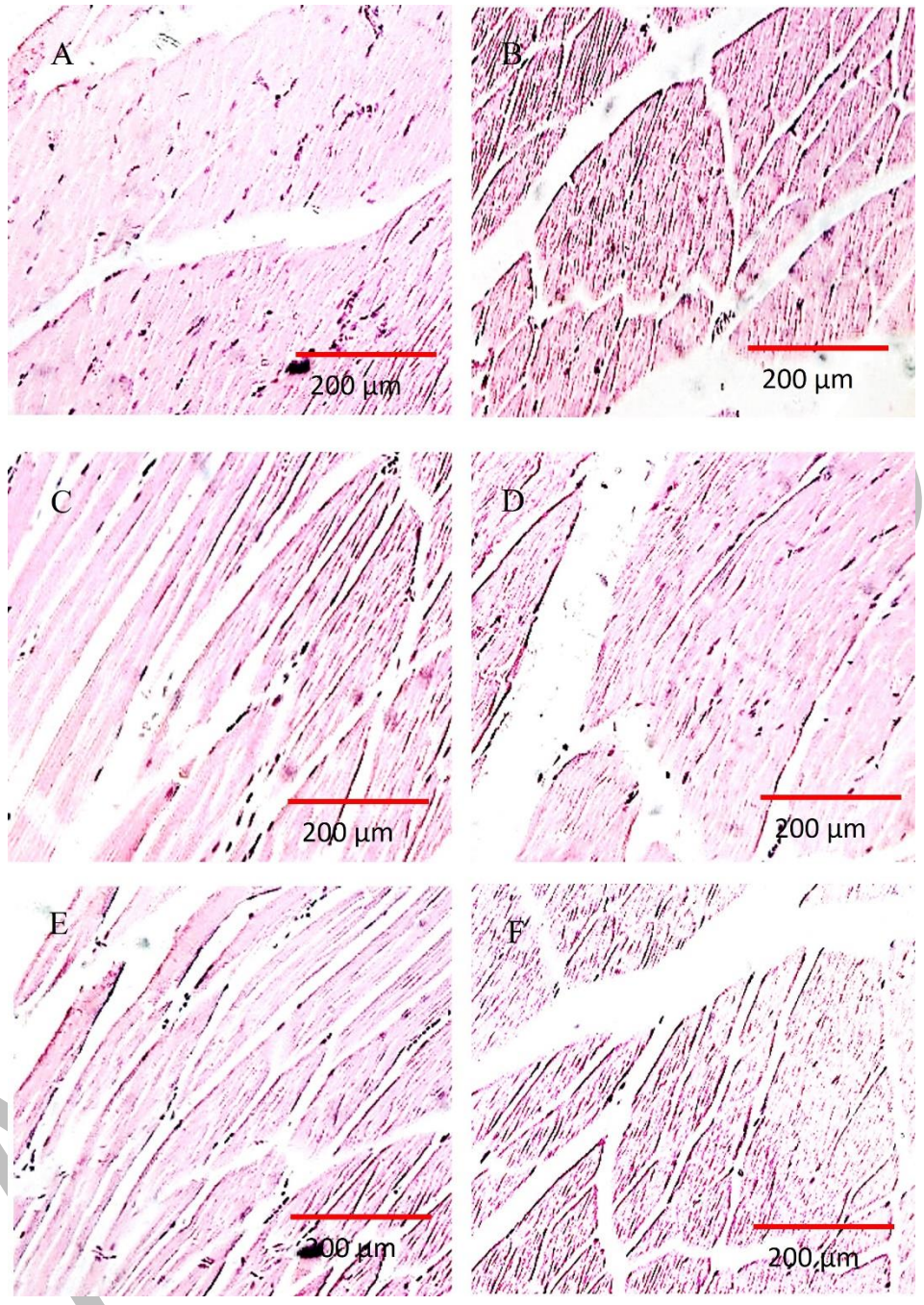

Figure 8. Masson's trichrome staining images of gastrocnemius muscle tissue in (A) autograft group, (B) GBEPCLGELADSCs + physical activity group, (C) GBEPCLGELADSCs group (D) PCLGEL + physical activity group, (E) PCLGEL group, and (F) negative control group

3-10. Functional assessment results

Results of SFI assessment (Figure 9 A) showed that the autograft group had significantly higher SFI scores than all other groups, p-value < 0.05. At week 8, SFI values for the animals treated

with GBEPCLGELADSCs + physical activity was significantly higher than GBEPCLGELADSCs, PCLGEL + physical activity, PCLGEL, and negative control groups, p-value < 0.05. Gastrocnemius muscle wet weight loss analysis (Figure 10 B) showed that muscular atrophy in the autograft group was significantly lower than GBEPCLGELADSCs, PCLGEL + physical activity, PCLGEL, and negative control groups, p-value < 0.05. However, the differences between the autograft and GBEPCLGELADSCs + physical activity groups were not significant, p-value > 0.05. Hotplate latency test (Figure 10 C) showed that the reaction time of the animals in autograft and GBEPCLGELADSCs + physical activity groups was significantly faster than other experimental groups, p-value < 0.05. Differences between autograft and GBEPCLGELADSCs + physical activity groups were not significant, p-value > 0.05.

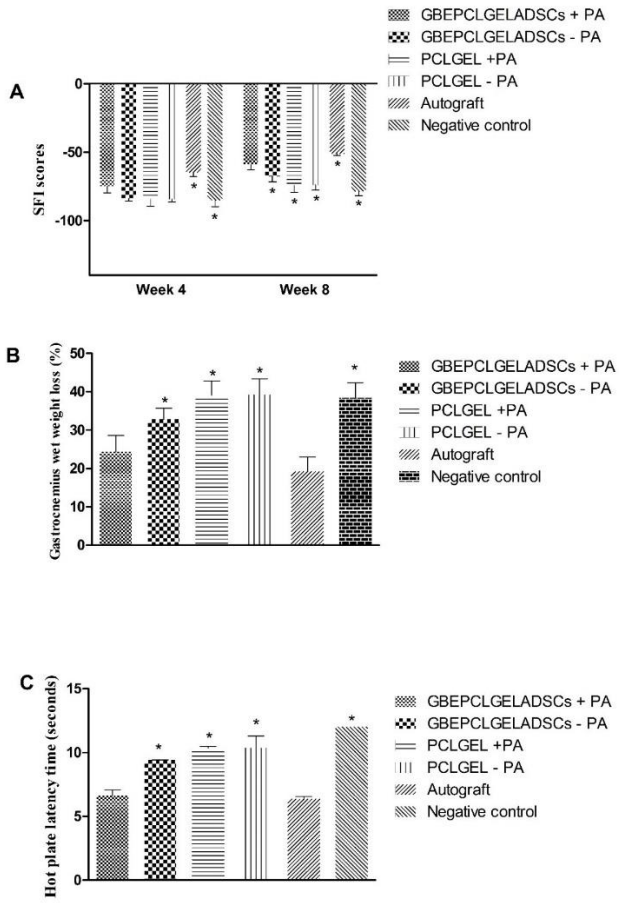

Figure 9. Functional assessment results showing (A) Sciatic function index, (B) gastrocnemius muscle wet weight loss, and (C) hot plate latency test in the animals treated with different treatment strategies. * Shows p-value < 0.05 relative to GBEPCLGELADSCs + PA group

3-11. ELISA assay

Results (Figure 10) showed that NGF and BDNF concentrations in GBEPCLGELADSCs + physical activity group was significantly higher than GBEPCLGELADSCs, PCLGEL + physical activity, PCLGEL, and negative control groups, p-value < 0.05. However, the autograft group had significantly higher concentrations of these proteins, p-value < 0.05.

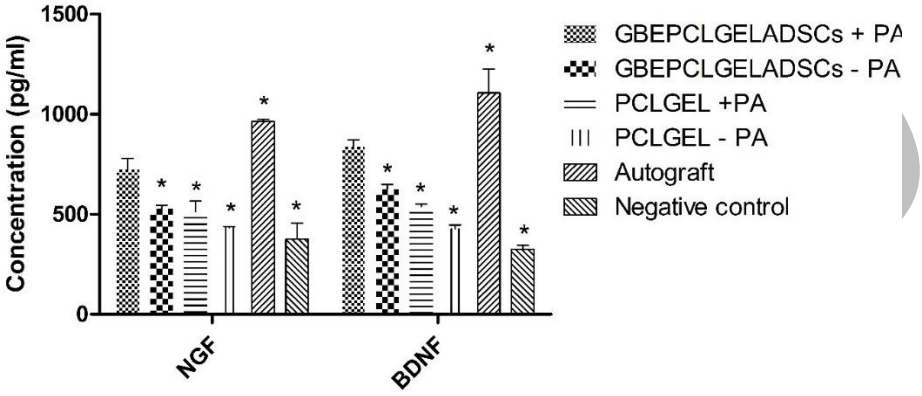

Figure 10. Concentrations of NGF and BDNF in animals in different experimental groups, * shows p-value < 0.05 relative to GBEPCLGELADSCs + PA group

4. Discussion

The repair and regeneration of the peripheral nervous system after damage or disease remains a significant challenge in neurosurgery. However, recent progress in tissue engineering approaches have shown promising results to repair the injuries through the utilization of electrospun delivery vehicles capable of delivering cells and therapeutic agents. This technology provides a three-dimensional matrix that mimics the native ECM of nervous system, improving various cellular functions [24-26]. In the current research, we developed a delivery system for GBE and ADSCs via an electrospun PCL/gelatin scaffolds. The microstructure of these constructs was typical of electrospun matrices. This fibrous structure has been shown to serve as a platform on which cells can adhere and promote the nervous system repair. Farzamfar et al. showed that electrospun PCL/gelatin scaffolds could successfully delivery unrestricted somatic stem cells at the site of PNS injury and improved the functional outcome [11]. The biocompatibility of our developed scaffolds was confirmed via the MTT assay. Indeed, both PCL and gelatin have been widely explored for various biomedical applications and their biocompatibility have been shown before [5,27, 32, 34,

]. This result ensures that our developed constructs offer a safe and effective platform for delivering cells and therapeutic agents to promote PNS regeneration and functional recovery. The modulation of the immune system plays a fundamental role in PNS regeneration as it regulates the inflammatory response, which can have both beneficial and detrimental effects on the healing outcomes. By modulating the immune reactions, it is possible to improve tissue repair, prevent scar formation, and establish a conducive condition for axonal sprouting, ultimately enhancing the chances of successful PNS repair and functional recovery [12, 22, 23, 26]. We showed that GBE improved scaffolds anti-inflammatory activity. It has been shown that several active compounds found in GBE, such as flavonoids and terpenoids contribute to its anti-inflammatory effects. Tao et al. showed that Biflavones in GBE decreased the expression of the Akt and p38 pathways in A549 cells. In addition, these substances also downregulated MUC5AC mRNA expression in A549 cells and the allergic mouse model [36]. Tensile properties of neural conduits is essential for their easy manipulation and suturing at the injury site. The high tensile properties of PCL/gelatin electrospun scaffolds can be attributed to the presence of PCL in the scaffolds. PCL, known for its robust mechanical properties, reinforces the scaffold's structure, enabling it to withstand the mechanical forces encountered during implantation and subsequent healing process [15, 17, 38]. The biodegradation of polymeric neural conduits should keep up with the pace of nervous system repair. Extremely high or low biodegradation rate compromises the healing process [39]. Our results confirmed the biodegradation rate of our developed scaffolds. Even after 60 days of incubation in PBS, the scaffold still kept their structural integrity. Initially, water molecules penetrate through the scaffolds, resulting in the hydrolysis of ester bonds present in PCL or other chemical bonds in gelatin. This process causes the polymeric chains to break down, resulting in the gradual biodegradation process. Generally, PCL possess a hydrophobic surface, making it unfavorable for cells adhesion. By blending gelatin with PCL the its surface hydrophobicity is modulated and increase the cells tendency towards this polymer [2]. Gelatin in PCL/gelatin scaffolds introduces carboxyl, amine, and hydroxyl groups, enhancing interaction with biological systems. Carboxyl groups allow chemical modifications and cross-linking. Amine groups promote cellular adhesion and proliferation, aiding tissue regeneration. Hydroxyl groups improve water absorption, facilitating cell signaling. These functional groups in PCL/gelatin scaffolds enhance biocompatibility and integration with biological systems for PNS tissue engineering [1, 9, 10, 40]. Release of GBE from GBEPCLGEL scaffolds can be explained by diffusion, biodegradation,

and swelling mechanisms [13, 41, 24, 46]. Overall therapeutic potential of GBEPCLGELADSCs + physical activity group was higher than other experimental groups. It could be that the synergistic healing potential of GBE, ADSCs, and physical activity has been involved in the healing effects of the treatment strategy. GBE possesses neuroprotective and antioxidant properties. Its active compounds, such as flavonoids and terpenoids, have been shown to stimulate nerve cell growth, reduce inflammation, and protect against nerve damage [33]. By providing a favorable environment for nerve regeneration, GBE can enhance the repair process. However, little data is available in literature to elucidate the mechanism behind the neuroprotective effects of GBE. On the other hand, ADSCs are an ideal cell source for nerve regeneration due to their multipotency and ability to differentiate into nerve cells. Once transplanted, ADSCs release growth factors and cytokines that promote nerve cell survival, axonal growth, and re-myelination. Their regenerative potential and ability to modulate the immune response contribute to the repair process [24, 46, 25]. Finally, engaging in physical activity is vital for the repair of the peripheral nervous system. Consistent exercise or rehabilitation exercises have a positive impact on blood circulation to the affected region, guaranteeing the supply of vital nutrients and oxygen required for nerve regeneration. Furthermore, physical activity triggers the release of growth factors and neurotrophic factors that aid in the survival of nerve cells, promote the growth of axons, and facilitate the establishment of functional connections between nerve cells [3, 14, 24, 25, 46]. This theory is in accordance with the results of ELISA assay. As shown, the NGF and BDNF concentrations in the GBEPCLGELADSCs + physical activity group was significantly higher than other groups that could be due to the effects of physical activity, GBE, or ADSCs. Additionally, it plays a crucial role in averting muscle atrophy and preserving muscle strength, thereby preventing potential complications.

5. Conclusion

In the course of this investigation, we innovatively crafted a hybrid methodology aimed at addressing peripheral nervous system injuries. Our examination focused on unraveling the synergistic healing capabilities arising from the combination of physical activity, ADSCs, and GBE in a rat model of sciatic nerve injury. The outcomes of our study revealed a noteworthy improvement in the recovery of both motor and sensory functions post-injury through the application of the hybrid approach. Delving deeper into the mechanistic aspects, our ELISA assay

hinted at a potential correlation between the observed healing effects and an elevated presence of NGF and BDNG concentrations in the sciatic nerve tissues. The extracellular vesicles produced by ADSCs and neuroprotective compounds in GBE may explain the upregulation of NGF and BDNF. Future research should extend the hybrid approach's potential by investigating synergies with other therapies, delving into molecular mechanisms using advanced techniques like single-cell RNA sequencing, and exploring the impact on neuro-immunological responses. Biomaterial integration, safety assessments, and population-specific considerations are paramount for comprehensive understanding and clinical applicability.

References

[1] Al Kury L.T., Dayyan F., Ali Shah F., Malik Z., Khalil A.A., Alattar A., Alshaman R,Ali A, Khan Z. Ginkgo biloba extract protects against methotrexate-induced hepatotoxicity: A computational and pharmacological approach. Molecules, 2020, 25, pp.25-40. DOI: 10.3390/molecules25112540

[2] Arif Z.U., Khalid M.Y., Noroozi R., Sadeghianmaryan A,Jalalvand M, Hossain M. Recent advances in 3d-printed polylactide and polycaprolactone-based biomaterials for tissue engineering applications. Int. J. Biol. Macromol., 2022,14, pp120-135. DOI: 10.1016/j.ijbiomac.2022.07.140

[3] Armada-da-Silva P.A.,Pereira C.,Amado S.,Veloso A.P. Role of physical exercise for improving posttraumatic nerve regeneration. Int. Rev. Neurobiol., 2013,, 109, pp.125-149. DOI: 10.1016/B978-0-12-420045-6.00006-7

[4] Bonaventura G ,Incontro S, Iemmolo R ,La Cognata V, Barbagallo I ,Costanzo E ,Barcellona M.L., Pellitteri R. ,Cavallaro S. Dental mesenchymal stem cells and neuro-regeneration: A focus on spinal cord injury. Cell Tissue Res., 2020, 379, pp.421-438. DOI: 10.1007/s00441-019-03109-4

[5] Carriel V, Alaminos M, Garzón I, Campos A, Cornelissen M. Tissue engineering of the peripheral nervous system. Expert Rev. Neurother., 2014, 14, pp.301-318. DOI: 10.1586/14737175.2014.887444

[6] Cobianchi S., Arbat-Plana A., Lopez-Alvarez V ,Navarro X. Neuroprotective effects of exercise treatments after injury: The dual role of neurotrophic factors. Curr. Neuropharmacol., 2017,15, pp.495-518. DOI: 10.2174/1570159X14666160330105132

[7] Dong M.M.,Yi T.H.,Stem cell and peripheral nerve injury and repair. Facial Plast. Surg., 2010, 26, pp.421-428. DOI: 10.1055/s-0030-1265023

[8] Dong R , Liu C,Tian S,Bai J,Yu K, Liu L, Tian, D, Electrospun polycaprolactone (pcl)-amnion nanofibrous membrane prevents adhesions and promotes nerve repair in a rat model of sciatic nerve compression. PLoS One, .2020, 15, pp.15-31. DOI: https://doi.org/10.1371/journal.pone.0244301

[9] Duymaz B.T., Erdiler F.B., Alan T, Aydogdu M.O., Inan A.T., Ekren N, Uzun M.,Sahin Y. M.,Bulus E, Oktar F.N. 3d bio-printing of levan/polycaprolactone/gelatin blends for bone tissue engineering: Characterization of the cellular behavior. Eur. Polym. J. , 2019,119, pp.426-437.DOI: https://doi.org/10.1016/j.eurpolymj.2019.08.015

[10] Echave M, Burgo L, Pedraz J ,Orive G. Gelatin as biomaterial for tissue engineering. Curr. Pharm. Des., 2017,23, pp.3567-3584. DOI: 10.2174/0929867324666170511123101

[11] Farzamfar S, Ehterami A, Salehi M, Vaeez A, Atashi A,Sahrapeyma H. Unrestricted somatic stem cells loaded in nanofibrous conduit as potential candidate for sciatic nerve regeneration. J. Mol. Neurosci., 2019, 67, pp.48-61. DOI: 10.1007/s12031-018-1209-9

[12] Farzamfar S, Naseri-Nosar M , Samadian H, Mahakizadeh S,Tajerian R ,Rahmati M,Vaez A ,Salehi M. Taurine-loaded poly (ε-caprolactone)/gelatin electrospun mat as a potential wound dressing material: In vitro and in vivo evaluation. J. Bioact. Compat. Polym., 2018,33, pp.282-294. https://doi.org/10.1177/0883911517737l0

[13] Hadjiargyrou M, Chiu J.B. Enhanced composite electrospun nanofiber scaffolds for use in drug delivery. Expert Opin. Drug Deliv., .2008, 5, pp.1093-1106. DOI: 10.1517/17425247.5.10.1093

[14] Houlton J, Abumaria N, Hinkley S.F., Clarkson A.N. Therapeutic potential of neurotrophins for repair after brain injury: A helping hand from biomaterials. Front. Neurosci., 2019,13, pp.790-805. DOI: 10.3389/fnins.2019.00790

[15] Houshyar S., Bhattacharyya A.,Shanks R.,Peripheral nerve conduit: Materials and structures. ACS Chem. Neurosci., 2019, 10, pp.349-365. DOI: https://doi.org/10.1021/acschemneuro.9b00203

[16] Huang W ,Ma,Y.X.,Fan Y.B., Lai S.M.,Liu H.Q.,Liu J., Luo L., Li G.Y.,Tian S.M. Extract of ginkgo biloba promotes neuronal regeneration in the hippocampus after exposure to acrylamide. Neural Regen. Res., 2017,12, pp.12-34. DOI: 10.4103/1673-5374.213548

[17] Jeong H, Rho J, Shin J.Y.,Lee D.Y., Hwang T, Kim K.J. Mechanical properties and cytotoxicity of pla/pcl films. Biomed. Eng. Lett., 2018,8, pp.267-282. DOI: 10.1007/s13534-018-0065-4

[18] Lavorato A , Raimondo S , Boido M ,Muratori L, Durante G, Cofano F,Vincitorio F,Petrone S,Titolo P,Tartara F. Mesenchymal stem cell treatment perspectives in peripheral nerve regeneration: Systematic review. Int. J. Mol. Sci., 2021,22, pp.57-62. DOI: 10.3390/ijms22020572

[19] Lee S, Patel M, Patel R., Electrospun nanofiber nerve guidance conduits for peripheral nerve regeneration: A review. Eur. Polym. J., 2022,15,pp.111-125,DOI: https://doi.org/10.1016/j.eurpolymj.2022.111663

[20] Lee S.K.,Wolfe S.W. Peripheral nerve injury and repair. JAAOS-Journal of the American AAOS, 2000, 8, pp.243-252.

[21] Li X ,Guan Y, Li C , Zhang T, Meng F, Zhang J, Li J ,Chen S, Wang Q,Wang Y. Immunomodulatory effects of mesenchymal stem cells in peripheral nerve injury. Stem cell res. ther., 2022,13, pp.1-13. DOI: https://doi.org/10.1186/s13287-021-02690-2

[22] Liu J.A., Yu J ,Cheung C W, Immune actions on the peripheral nervous system in pain. Int. J. Mol. Sci., 2021, 22, pp.14-48. DOI: 10.3390/ijms22031448

[23] Liu P, Peng J, Han G.H., Ding X.,Wei S.,Gao G.,Huang K.,Chang F.,Wang Y, Role of macrophages in peripheral nerve injury and repair. Neural Regen. Res., .2019,14, pp.13-35. DOI: 10.4103/1673-5374.253510

[24] Masgutov R, Masgutova G, Mullakhmetova A, Zhuravleva M, Shulman A, Rogozhin, A, Syromiatnikova V, Andreeva D ,Zeinalova A ,Idrisova K. Adipose-derived mesenchymal stem cells applied in fibrin glue stimulate peripheral nerve regeneration. Front. Med. 2019,6, pp.68-79. DOI: 10.3389/fmed.2019.00068

[25] Maugeri G, D'Agata V., Trovato B, Roggio F, Castorina A,Vecchio M ,Di Rosa M ,Musumeci G. The role of exercise on peripheral nerve regeneration: From animal model to clinical application. Heliyon, 2021, 7, pp20-45. DOI: 10.1016/j.heliyon.2021.e08281

[26] Mietto B.S., Mostacada K., Martinez A.M. Neurotrauma and inflammation: Cns and pns responses. Mediators Inflamm., 2015, 2015, pp21-36. DOI: 10.1155/2015/251204

[27] Naseri-Nosar M ,Farzamfar S,Sahrapeyma H, Ghorbani S.,Bastami F,Vaez A, Salehi M Cerium oxide nanoparticle-containing poly (ε-caprolactone)/gelatin electrospun film as a

potential wound dressing material: In vitro and in vivo evaluation. Mater. Sci. Eng. C , 2017,81, pp.366-372. DOI: 10.1016/j.msec.2017.08.013

[28] O'brien F J. Biomaterials & scaffolds for tissue engineering. Mater Today, 2011,14, pp.88-95. DOI: https://doi.org/10.1016/S1369-7021(11)70058-X

[29] Oliveira J.T., De C., Lima S.V.S., Mendonça H.R., Andrade K.M.,Baptista A.F., Martinez A. M., Peripheral nervous system: Regenerative therapies. Regenerative Medicine-from Protocol to Patient: 4. Regen. Ther. , 2016, 12 pp.147-178. DOI:https://doi.org/10.1007/978-3-319-28293-0

[30] Park J.S., Höke A. Treadmill exercise induced functional recovery after peripheral nerve repair is associated with increased levels of neurotrophic factors. PLoS One, 2014, 9, pp 156-165, DOI: 10.1371/journal.pone.0090245

[31] Roseti L , Parisi V, Petretta M ,Cavallo C, Desando G, Bartolotti I, Grigolo B. Scaffolds for bone tissue engineering: State of the art and new perspectives. Mater. Sci. Eng. C, 2017,78, pp.246-262. DOI: 10.1016/j.msec.2017.05.017

[32] Shahbazi E, Kiani S, Gourabi H, Baharvand H. Electrospun nanofibrillar surfaces promote neuronal differentiation and function from human embryonic stem cells. Tissue Eng. Part A, 2011,17, pp.21-31. DOI: 10.1089/ten.TEA.2011.0121

[33] Singh S.K., Srivastav S, Castellani R.J., Plascencia-Villa G.,Perry G. Neuroprotective and antioxidant effect of ginkgo biloba extract against ad and other neurological disorders. Neurotherapeutics, .2019,16, pp.66-74. DOI: 10.1007/s13311-019-00767-8

[34] Smith A.S.,Passey S.L.,Martin N.R.,Player D.J.,Mudera V.,Greensmith L ,Lewis M.P. Creating interactions between tissue-engineered skeletal muscle and the peripheral nervous system. Cells Tissues Organs, 2016,, 202, pp.143-158. DOI: 10.1159/000443634

[35] Sullivan R, Dailey T, Duncan K, Abel N, Borlongan C .V. Peripheral nerve injury: Stem cell therapy and peripheral nerve transfer. Int. J. Mol. Sci., 2016,17, pp.21-33. doi: 10.3390/ijms17122101

[36] Tao Z, Jin W, Ao M, Zhai S, Xu H ,Yu L, Evaluation of the anti-inflammatory properties of the active constituents in ginkgo biloba for the treatment of pulmonary diseases. Food Funct, .2019, 10, pp.209-220. DOI: 10.1039/c8fo02506a

[37] Taylor C.S., Haycock J.W., Biomaterials and scaffolds for repair of the peripheral nervous system. J Tissue Eng Regen Med., 2022, 20, pp.245-279. DOI: https://doi.org/10.1007/978-3-030-06217-0_3-1

[38] Van Opstal N,Feyen H, Luyckx J, Bellemans J, Mean tensile strength of the pcl in tka depends on the preservation of the tibial insertion site. Knee Surg. Sports Traumatol. Arthrosc., 2016,24, pp.273-288. DOI: 10.1007/s00167-014-3377-7

[39] Vijayavenkataraman S, Nerve guide conduits for peripheral nerve injury repair: A review on design, materials and fabrication methods. Acta Biomater., .2020,106, pp.54-69. DOI: 10.1016/j.actbio.2020.02.003

[40] Yazdanpanah A , Madjd Z, Pezeshki-Modaress M, Khosrowpour Z, Farshi P, Eini L, Kiani J ,Seifi M, Kundu S.C., Ghods R. Bioengineering of fibroblast-conditioned polycaprolactone/gelatin electrospun scaffold for skin tissue engineering. Artif. Organs, 2022, 46, pp.1040-1054. DOI: 10.1111/aor.14169

[41] Ye K, Kuang H,You Z, Morsi Y, Mo X. Electrospun nanofibers for tissue engineering with drug loading and release. Pharmaceutics, 2019,11, pp.182-193. DOI: 10.3390/pharmaceutics11040182

[42] Yi S, Zhang Y, Gu X, Huang L, Zhang K , Qian T, Gu X. Application of stem cells in peripheral nerve regeneration. Burns Trauma, 2020, 8, pp 15-32. DOI: 10.1093/burnst/tkaa002

[43] Yousefi F , Arab F.L., Nikkhah K ,Amiri H , Mahmoudi M. Novel approaches using mesenchymal stem cells for curing peripheral nerve injuries. Life Sci., 2019,221, pp.99-108. DOI: 10.1016/j.lfs.2019.01.052

[44] Zhang J, Liu Y, Chen Y, Yuan L, Liu H, Wang J, Liu Q, Zhang Y. Adipose-derived stem cells: Current applications and future directions in the regeneration of multiple tissues. Stem Cells Int ,2020, 11, pp 23-39. DOI: 10.1155/2020/8810813

[45] Zhang P.X., Han N., Kou Y.H., Zhu Q.T.,Liu X.L.,Quan D.P.,Chen J.G., Jiang B.G.,Tissue engineering for the repair of peripheral nerve injury. Neural Regen. Res., 2019, 14, pp.51-69. DOI: 10.4103/1673-5374.243701

[46] Zhang R.C., Du W.Q., Zhang J.Y.,Yu S.X.,Lu F.Z.,Ding H.M.,Cheng Y.B., Ren C.,Geng D.Q. Mesenchymal stem cell treatment for peripheral nerve injury: A narrative review. Neural Regen. Res., 2021,16, pp.210-231. DOI: 10.4103/1673-5374.310941

[47] Zochodne D.,Levy D.,Nitric oxide in damage, disease and repair of the peripheral nervous system. Cell. Mol. Biol., 2005, 51, pp.255-267.